

Quantum phase transition in a two-channel-Kondo quantum dot device

M. Pustilnik,¹ L. Borda,^{2,3} L. I. Glazman,⁴ and J. von Delft²

¹*School of Physics, Georgia Institute of Technology, Atlanta, Georgia 30332, USA*

²*Sektion Physik and Center for Nanoscience, LMU München, Theresienstrasse 37, 80333 München, Germany*

³*Hungarian Academy of Sciences, Institute of Physics, TU Budapest, H-1521, Hungary*

⁴*William I. Fine Theoretical Physics Institute, University of Minnesota, Minneapolis, Minnesota 55455, USA*

(Received 29 September 2003; published 15 March 2004)

We develop a theory of electron transport in a double quantum dot device recently proposed in [Y. Oreg and D. Goldhaber-Gordon, *Phys. Rev. Lett.* **90**, 136602 (2003)] for the observation of the two-channel Kondo effect. Our theory provides a strategy for tuning the device to the non-Fermi-liquid fixed point, which is a quantum critical point in the space of device parameters. We explore the corresponding quantum phase transition, and make explicit predictions for behavior of the differential conductance in the vicinity of the quantum critical point.

DOI: 10.1103/PhysRevB.69.115316

PACS number(s): 72.15.Qm, 73.23.Hk, 73.63.Kv

I. INTRODUCTION

The magnetic screening of a localized spin by spins of itinerant electrons¹ leads to the Kondo effect—an anomaly in low-temperature conduction properties. This screening becomes effective below some characteristic temperature, the Kondo temperature T_K . Above T_K electrons are weakly scattered by the magnetic impurity, but below T_K the scattering becomes strong. In the simplest Kondo systems, only one electron mode (the s -wave mode, say) participates in the screening of a localized spin with $S=1/2$. In this case, the low-temperature electronic properties are adequately described by Fermi liquid theory,² and the thermodynamic and transport characteristics are analytical functions of T/T_K . In more complicated systems (such as, e.g., paramagnetic metals) many electron modes may participate in screening of an $S=1/2$ localized moment.³ The peculiarities of such a “multichannel” Kondo model were long recognized.^{3,4} At the same time it was understood that even a small deviation from symmetry between channels leads at low temperatures to the Kondo screening by just one channel, the one for which the exchange integral with the impurity is the largest.⁴

The peculiarity of a *symmetric* multichannel Kondo problem is in its non-Fermi-liquid (NFL) behavior at low temperatures.⁴ The low-temperature asymptotes of the thermodynamic and transport characteristics display power-law behavior with fractional values of the exponents. A complete temperature dependence of the thermodynamic characteristics (such as the local spin susceptibility) is known now from the exact Bethe-ansatz solution of the Kondo problem.^{5,6} Details of the low-temperature electron scattering problem were also understood in the framework of conformal field theory.^{7,8}

Experimental observation of the non-Fermi-liquid behavior in a Kondo system, however, is difficult because the channel symmetry is not “protected”—in general, there are no conservation laws prescribing such a symmetry. This has led to various propositions to observe such a behavior in systems where the role of spin is taken over by another degree of freedom, while the “real” spin labels the channels, making the channel symmetry robust. One such idea deals

with an atomic defect which occupies two equivalent lattice sites, thus forming a pseudospin.⁹ However, the equivalence of sites is not a protected symmetry; its violation,¹⁰ equivalent to a “Zeeman splitting” of the pseudospin states, destroys the Kondo effect.

Another object which under certain conditions can be described by the two-channel Kondo model (2CK) model, is a large quantum dot, or a metallic island connected by a single-mode channel to a conducting electrode.¹¹ If one neglects the finite level spacing in the island, then a pseudospin labeling of the charge states of the island may be introduced, while real spin again plays the part of the channel index. In this setup the degeneracy with respect to the pseudospin orientation is easily achieved by tuning the gate voltage to the vicinity of the Coulomb blockade degeneracy point. At temperatures T higher than the level spacing δE in the island, the system is then described by the 2CK model.¹¹ Since T_K for this system can be of the order¹² of the charging energy E_C , while typically $\delta E \ll E_C$, the NFL regime is easily realized. When an additional electrode is attached to the island, one can study the transport properties of the resulting device. The disadvantage of such realization of a 2CK system is that there is no mapping between the conductance across the island¹³ and the electron scattering cross-section in the generic two-channel Kondo model.^{7,8}

Small quantum dots with large level spacing have proved to be suitable for the observation of the Kondo effect.¹⁴ In the usual geometry consisting of a dot with two attached electrodes, however, only the conventional Fermi-liquid (FL) behavior is observable at low temperatures. The reason lies in the structure of the matrix of exchange constants that couple the dot’s spin to the spins of itinerant electrons.^{15,16} Typically, the eigenvalues of this matrix are vastly different,¹⁵ and their ratio is not tunable by conventional means.

A device that circumvents this problem was proposed recently in Ref. 17, and involves several dots. A two-dot device is sufficient for the realization of the 2CK model. The key idea of Ref. 17 is to replace one of the electrodes in the standard configuration by a very large quantum dot 2, see Fig. 1, characterized by a level spacing δE_2 and a charging

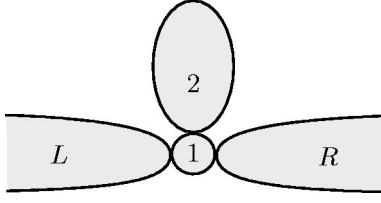


FIG. 1. Device proposed in Ref. 17. Level spacing in the larger dot (2) must be negligibly small to allow for the NFL behavior of the device at low temperatures.

energy E_2 . At $T \gg \delta E_2$, particle-hole excitations within this dot are allowed, and electrons of dot 2 participate in the screening of the smaller dot's spin. At the same time, as long as $T \ll E_2$, the number of electrons in the dot 2 is fixed. As a result, the electrons in dot 2 provide for a separate channel which does not mix with the channels provided by the electrodes L and R . In this case, the exchange constants for two channels may be tuned to become equal:¹⁷ the asymmetry between the channels is controlled by the ratio of the conductances of the dot leads and dot-dot junctions.

In principle, a setup having just one lead and two dots would allow one to study thermodynamic properties, such as magnetic susceptibility, in the 2CK regime. The existing technology,¹⁴ however, enables one to measure transport rather than thermodynamic properties. Therefore, two leads are needed to perform conductance measurements. In this paper, we assume that one of the electrodes is coupled weakly to the small dot and serves as a probe of the 2CK system formed by the two dots and the remaining electrode. We propose a detailed strategy for tuning the device to the NFL regime, and discuss various manifestations of NFL-related physics in the transport properties of the system.

II. THE MODEL

According to the discussion above, the device we consider consists of two quantum dots coupled to two conducting leads via single-mode junctions. The model Hamiltonian of such a device can be written as a sum of three parts

$$H = H_d + H_l + H_t. \quad (1)$$

The first term here, H_d , describes an isolated system of two quantum dots, 1 and 2, connected via a single mode junction

$$H_d = E_1 \left(\sum_s d_s^\dagger d_s - N \right)^2 + \sum_{ks} \xi_k \psi_{2ks}^\dagger \psi_{2ks} + E_2 \left(\sum_{ks} \psi_{2ks}^\dagger \psi_{2ks} \right)^2 + \sum_{ks} (t_2 \psi_{2ks}^\dagger d_s + \text{H.c.}). \quad (2)$$

The last two terms in Eq. (1) represent the free electrons with spin $s = \pm 1$ in leads R and L , and the tunneling between the leads and dot 1, see Fig. 1,

$$H_l = \sum_{aks} \xi_k c_{aks}^\dagger c_{aks}, \quad \alpha = R, L; \quad (3)$$

$$H_t = \sum_{aks} t_\alpha c_{aks}^\dagger d_s + \text{H.c.} \quad (4)$$

In Eq. (2) the smaller dot (dot 1) is described by a single-level system equivalent to the Anderson impurity model. The parameter E_1 represents charging energy, while the parameter N is adjustable by tuning the potential on the capacitively coupled gate electrode. We neglect the finite level spacing δE_2 in the dot 2, but account for its finite charging energy E_2 (we do not write explicitly the gate potential applied to the dot 2, as it corresponds to a trivial shift of the chemical potential).

Since the relevant energies ($\omega \lesssim T_K$) for the Kondo effect are negligibly small compared to the Fermi energy, the electronic dispersion relation ξ_k in Eqs. (2), (3) can be linearized: $\xi_k = v_F k$, where k is measured from the Fermi momentum k_F . The linearization leads to an energy-independent density of states ν , which will be assumed throughout this paper. Finally, we treat the tunneling amplitudes t_2, t_R, t_L as real numbers and neglect their dependences on k . This is well justified for relevant values of k , $|k| \lesssim T/v_F$.

Instead of working with the operators $c_{R,L}$, it is convenient to introduce their linear combinations $\psi_{0,1}$,

$$\begin{pmatrix} \psi_{1ks} \\ \psi_{0ks} \end{pmatrix} = \begin{pmatrix} \cos \theta_0 & \sin \theta_0 \\ -\sin \theta_0 & \cos \theta_0 \end{pmatrix} \begin{pmatrix} c_{Rks} \\ c_{Lks} \end{pmatrix}, \quad (5)$$

where the angle θ_0 is determined by the equation

$$\tan \theta_0 = t_L / t_R. \quad (6)$$

(So far there are no restrictions on the value of t_L/t_R .) The Hamiltonian (1)–(4) then assumes the “block-diagonal” form

$$H = H_0 \{ \psi_0 \} + H_1 \{ \psi_1, \psi_2, d \}, \quad (7)$$

$$H_0 = \sum_{ks} \xi_k \psi_{0ks}^\dagger \psi_{0ks}, \quad (8)$$

$$H_1 = H_d \{ \psi_2, d \} + \sum_{ks} \xi_k \psi_{1ks}^\dagger \psi_{1ks} + \sum_{ks} (t_1 \psi_{1ks}^\dagger d_s + \text{H.c.}), \quad (9)$$

where $H_d \{ \psi_2, d \}$ is given by Eq. (2), and $t_1 = \sqrt{t_L^2 + t_R^2}$.

At low energies ($T \ll E_{1,2}$) the Hamiltonian H_1 involving the ψ_1 and ψ_2 operators, see Eq. (9), can be simplified further. Indeed, at $N \approx 1$ the small dot is occupied by a single electron, and, therefore, carries a spin $S = 1/2$. The tunneling terms in Eqs. (2) and (9) mix the states with a single electron in dot 1 with states having 0 or 2 electrons in that dot. Because of the high energy cost ($\sim E_1$), these transitions are virtual, and, provided that the conductances of the corresponding junctions are small, can be taken into account perturbatively in the second order in tunneling amplitudes. A new¹⁷ and important element here compared to the conventional treatment of the Anderson impurity model is that at $T \ll E_2$ only those excitations that conserve the number of electrons in dot 2 are allowed. The resulting effective Hamil-

tonian which acts within the strip of energies $|\omega| \lesssim \min\{E_1, E_2\}$, has the form of the 2CK model,⁴⁻⁹

$$H_{2\text{CK}} = \sum_{\gamma ks} \xi_k \psi_{\gamma ks}^\dagger \psi_{\gamma ks} + \sum_{\gamma} J_{\gamma} (\mathbf{s}_{\gamma} \cdot \mathbf{S}) + BS^z. \quad (10)$$

Here the channel index $\gamma=1$ and $\gamma=2$ represents the leads and dot 2, respectively, \mathbf{S} is the spin-1/2-operator describing the doubly-degenerate ground state of dot 1,

$$\mathbf{s}_{\gamma} = \sum_{kk's's'} \psi_{\gamma ks}^\dagger \frac{\boldsymbol{\sigma}_{ss'}}{2} \psi_{\gamma k's'}$$

is the spin density in channel γ , and $\boldsymbol{\sigma} = (\sigma^x, \sigma^y, \sigma^z)$ are the Pauli matrices. The exchange amplitudes J_{γ} in Eq. (10) are estimated as

$$\nu J_{\gamma} = 4\nu t_{\gamma}^2 / E_1. \quad (11)$$

In derivation of Eq. (10), we assumed that the gate voltage is tuned precisely to $N=1$ (which corresponds to a particle-hole symmetric situation). As we discuss in Sec. V below, this assumption does not lead to qualitative changes in the results. We also included in the Hamiltonian the effect of an external magnetic field (hereinafter we omit the Bohr magneton μ_B ; the field B is measured in the units of energy).

III. TUNNELING CONDUCTANCE

In order to study the out-of-equilibrium transport across the device we add to our Hamiltonian a term

$$H_V = \frac{eV}{2} (\hat{N}_L - \hat{N}_R), \quad \hat{N}_{\alpha} = \sum_{ks} c_{\alpha ks}^\dagger c_{\alpha ks}, \quad (12)$$

which describes a finite bias voltage V applied between the left ($\alpha=L$) and right ($\alpha=R$) electrodes. The differential conductance dI/dV can be evaluated in a closed form for arbitrary V when one of the leads, say L , serves as a weakly coupled probe,¹⁶ i.e., $t_L \ll t_R$. Under this condition the angle θ_0 in Eqs. (5) and (6) is small:

$$\theta_0 \approx t_L / t_R \ll 1. \quad (13)$$

Application of the transformation Eq. (5) to Eq. (12), yields, to the linear order in θ_0 ,

$$H_V = \frac{eV}{2} (\hat{N}_0 - \hat{N}_1) + eV\theta_0 \sum_{ks} (\psi_{0ks}^\dagger \psi_{1ks} + \text{H.c.}), \quad (14)$$

where

$$\hat{N}_0 = \sum_{ks} \psi_{0ks}^\dagger \psi_{0ks}, \quad \hat{N}_1 = \sum_{ks} \psi_{1ks}^\dagger \psi_{1ks}.$$

The first term on the right-hand side of Eq. (14) can be interpreted as a voltage bias between the reservoirs of 0 and 1 particles, cf. Eq. (12), while the second term has an appearance of the k -conserving tunneling. Since the tunneling am-

plitude is proportional to the small parameter $\theta_0 \ll 1$, see Eq. (13), one can use perturbation theory to calculate the current across the device.¹⁶

Similar to the representation of H_V in the form of Eq. (14), the current operator

$$\hat{I} = \frac{d}{dt} \frac{e}{2} (\hat{N}_R - \hat{N}_L)$$

also splits naturally into two contributions,

$$\hat{I} = \hat{I}_0 + \delta\hat{I}. \quad (15)$$

Here

$$\hat{I}_0 = \frac{d}{dt} \frac{e}{2} (\hat{N}_1 - \hat{N}_0) = ie^2 V \theta_0 \sum_{ks} \psi_{0ks}^\dagger \psi_{1ks} + \text{H.c.}, \quad (16)$$

is a current between the reservoirs of 0 and 1 particles and

$$\delta\hat{I} = -e\theta_0 \frac{d}{dt} \sum_{ks} \psi_{0ks}^\dagger \psi_{1ks} + \text{H.c.} \quad (17)$$

It is easy to show¹⁶ that in the leading (second) order in θ_0 the operator $\delta\hat{I}$ does not contribute to the average current across the device. The remaining contribution $\langle \hat{I}_0 \rangle$ corresponds to the k -conserving tunneling between two bulk reservoirs containing 0 and 1 particles, see Eqs. (14) and (16). Its evaluation yields¹⁶

$$\frac{dI}{dV} = G_0 \sum_s \frac{1}{2} \int d\omega (-df/d\omega) [-\pi\nu \text{Im} T_{1s}(\omega + eV)] \quad (18)$$

for the differential conductance. Here $f(\omega)$ is the Fermi function (ω is the energy measured from the Fermi level),

$$G_0 = \frac{2e^2}{h} (2\theta_0)^2 \approx \frac{8e^2}{h} \frac{t_L^2}{t_R^2}, \quad (19)$$

and T_{1s} is the t-matrix for the particles of channel $\gamma=1$ [evaluated with the equilibrium Hamiltonians (9) or (10)]. The t-matrix is related to the exact retarded Green function $G_{ks, k's'} = \delta_{ss'} G_{ks, k's}$ of these particles according to

$$G_{ks, k's} = G_k^0 + G_k^0 T_{1s}^0 G_{k'}^0, \quad G_k^0 = (\omega - \xi_k + i0)^{-1}.$$

Here we took into account the conservation of the total spin, which implies that $G_{ks, k's'}$ is diagonal in s, s' . In our model with t_1 independent of k (and, consequently, J_1 independent of k and k'), the t-matrix is also independent of k, k' . Note that the linear response ($V \rightarrow 0$) counterpart of Eq. (18), the linear conductance

$$G = G_0 \sum_s \frac{1}{2} \int d\omega (-df/d\omega) [-\pi\nu \text{Im} T_{1s}(\omega)], \quad (20)$$

remains valid¹⁶ for an arbitrary relation between t_L and t_R , in which case $G_0 = (2e^2/h) \sin^2(2\theta_0)$.

IV. TRANSPORT AT FINITE TEMPERATURE AND BIAS

Equation (18) provides a direct link between the measurable quantity, the differential conductance dI/dV , and the properties of the 2CK model, Eq. (10). In the channel-symmetric case $J_1=J_2=J$ the NFL behavior manifests itself in a nonanalytic dependence of the t-matrix on energy and temperature,⁸ which leads to a rather unusual scaling of the differential conductance at low bias and temperature ($|eV|, T \ll T_K$):

$$\frac{1}{G_0} \frac{dI}{dV} = \frac{1}{2} \left[1 - \sqrt{\frac{\pi T}{T_K}} F_{2\text{CK}} \left(\frac{|eV|}{\pi T} \right) \right]. \quad (21)$$

The function $F_{2\text{CK}}(x)$ here is a universal (parameter-free) scaling function⁸ with the asymptotes

$$F_{2\text{CK}}(x) = \begin{cases} 1 + cx^2, & x \ll 1, \\ \frac{3}{\sqrt{\pi}} \sqrt{x}, & x \gg 1, \end{cases} \quad (22)$$

where c is a numerical coefficient of the order of 1. The limit $eV/T \rightarrow 0$ of Eq. (21) yields

$$G = G_0 \frac{1}{2} (1 - \sqrt{\pi T/T_K}) \quad (23)$$

for the linear conductance (this result is valid for arbitrary value of t_L/t_R). The estimate¹⁸ of the Kondo temperature T_K introduced in Eqs. (21) and (23) reads⁹

$$T_K \sim E_0 (\nu J) e^{-1/J\nu}, \quad E_0 = \min\{E_1, E_2\}. \quad (24)$$

The validity of Eqs. (21) and (23) is limited by the requirements that both the Zeeman energy B and the level spacing δE_2 are small compared to T , and that the exchange constants in Eq. (10) are equal to each other: $J_1=J_2$. When the system is tuned away from this special point, at a finite

$$\Delta = \nu J_1 - \nu J_2, \quad (25)$$

the conductance changes drastically. In the ideal case of $T=0$ and $\delta E_2=0$, the conductance has a steplike dependence on Δ ,

$$G(\Delta) = G_0 \theta(\Delta). \quad (26)$$

The discontinuity in Eq. (26) reflects a *quantum phase transition* between two different Fermi liquid (FL) states, in which the spin of the dot 1 forms a singlet with either the collective spin of the electrons in the leads (FL1, $\Delta > 0$) or with that of the dot 2 (FL2, $\Delta < 0$). At the critical point $\Delta = 0$, the system exhibits NFL behavior down to $T=0$. In agreement with the general theory of quantum phase transitions,¹⁹ the $T \rightarrow 0$ asymptotics at $|\Delta| \neq 0$ corresponds to the FL, whereas the NFL behavior (23) is preserved at temperatures well above certain Δ -dependent crossover scale T_Δ , see Fig. 2. By the same token, the step in the Δ dependence of $G(\Delta)$, Eq. (26), is smeared at finite temperatures.

In order to estimate¹⁸ the energy scale T_Δ we consider the renormalization group (RG) flow of the effective exchange

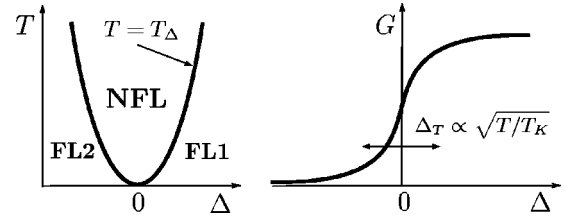


FIG. 2. Quantum phase transition between two FL states. The NFL behavior is preserved at $|\Delta| \neq 0$, provided the temperature exceeds the crossover scale T_Δ , see Eq. (31). The width Δ_T of step in the conductance $G(\Delta)$ scales with temperature as \sqrt{T} , see Eq. (34).

constants as the high-energy cutoff D is reduced from its initial value $D_0 \sim E_0$. We are interested in the case when the bare value of Δ is small,

$$|\Delta| \ll \mathcal{J},$$

where

$$\mathcal{J} = \nu(J_1 + J_2)/2. \quad (27)$$

The evolution of the effective coupling constants \mathcal{J}^*, Δ^* with the decrease of D is then described by the Poor Man's scaling equations¹

$$\frac{d\mathcal{J}^*}{d\zeta} = (\mathcal{J}^*)^2, \quad \frac{d\Delta^*}{d\zeta} = 2\mathcal{J}^*\Delta^*, \quad \zeta = \ln \frac{D_0}{D} \quad (28)$$

with the initial conditions

$$\mathcal{J}^*(D_0) = \mathcal{J}, \quad \Delta^*(D_0) = \Delta.$$

Equations (28) are valid as long as $\Delta^* \ll \mathcal{J}^* \ll 1$ and yield the relation $\Delta^*/\Delta = (\mathcal{J}^*/\mathcal{J})^2$. By the time \mathcal{J}^* has grown to be of the order of 1 at $D \sim T_K$, the value of Δ^* characterizing the channel asymmetry reaches

$$\Delta^*(T_K) \sim \Delta/\mathcal{J}^2. \quad (29)$$

This can be viewed as the initial (at $D \sim T_K$) value of the coupling constant of the relevant^{4,20} channel-symmetry-breaking perturbation. The perturbation will eventually drive the system away from the 2CK fixed point at $D \rightarrow 0$. However, if $\Delta^*(T_K) \ll 1$, then one expects the behavior of the system in a broad range of energies to be still governed by the vicinity of the 2CK fixed point. The channel anisotropy is a relevant operator with scaling dimension 1/2, see Ref. 20. Hence, the dependence of the corresponding coupling constant Δ^* on D is described by

$$\frac{\Delta^*(D)}{\Delta^*(T_K)} \propto \left(\frac{T_K}{D} \right)^{1/2}. \quad (30)$$

The condition $\Delta^*(T_\Delta) \sim 1$, together with Eq. (29), then gives the estimate

$$T_\Delta \sim [\Delta^*(T_K)]^2 T_K \sim (\Delta^2/\mathcal{J}^4) T_K. \quad (31)$$

The RG flow stops at $D \sim \max\{T, |eV|\}$. Consequently, at $\max\{T_\Delta, |eV|\} \ll T \ll T_K$, the channel asymmetry yields a small

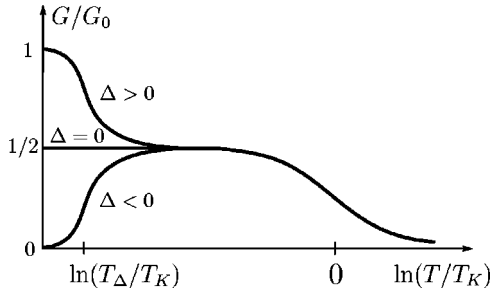


FIG. 3. Sketch of the temperature dependence of the linear conductance at fixed values of Δ and T_K . For $\Delta < 0$ the dependence is nonmonotonic, with a maximum at $T \sim \sqrt{T_\Delta T_K}$. At $T \gg T_K$ the conductance scales as $G/G_0 \propto [\ln(T/T_K)]^{-2}$, see, e.g., Ref. 16.

correction to the conductance Eq. (23). The correction is first order in the corresponding perturbation, hence proportional to $\Delta^*(T) \sim (T_\Delta/T)^{1/2}$, and its sign is determined by the sign of Δ :

$$\delta G/G_0 \propto \text{sgn}(\Delta) \left(\frac{T_\Delta}{T} \right)^{1/2}. \quad (32)$$

On the other hand, for $T, |eV| \ll T_\Delta$ the system is a Fermi liquid, see Fig. 2. Substitution of the t-matrix in the form

$$-\pi\nu \text{Im} T_{1s} = \theta(\Delta) - \text{sgn}(\Delta) \frac{3\omega^2 + \pi^2 T^2}{2T_\Delta^2}$$

(cf. Ref. 8) into Eq. (18) then yields

$$\frac{1}{G_0} \frac{dI}{dV} = \theta(\Delta) - \text{sgn}(\Delta) \left(\frac{\pi T}{T_\Delta} \right)^2 \left[1 + \frac{3}{2} \left(\frac{eV}{\pi T} \right)^2 \right]. \quad (33)$$

Again, the linear response ($V \rightarrow 0$) counterpart of Eq. (33) is valid at any ratio t_L/t_R . The temperature dependence of the linear conductance at fixed small values of Δ is sketched in Fig. 3.

According to Eq. (33), corrections to the zero-temperature limit of the linear conductance, the step function (26), are quadratic in temperature—a typical Fermi-liquid result.² At a finite temperature, the step function is smeared, see Fig. 2. The characteristic width Δ_T of the smeared step at temperature T is estimated by solving the equation $T_\Delta \sim T$ for Δ , which results in

$$\Delta_T \sim \mathcal{J}^2 \sqrt{T/T_K}. \quad (34)$$

This “sharpening” of the Δ dependence of the linear conductance with decreasing temperatures (see Fig. 2) can be regarded as a “smoking gun” for non-Fermi-liquid behavior. In fact, it might be easiest to first identify unambiguously the steplike dependence of the conductance on Δ and then use it to tune the device precisely to the symmetry point in order to observe the distinctive scaling of the differential conductance Eq. (21). Experimentally, the value of Δ is controlled¹⁷ by the asymmetry of the conductances of the corresponding tunneling junctions, which in turn are controlled by the potentials V_g on the gates forming the junctions. In the vicinity of the symmetry point, the dependence of G on V_g should have

the form of a smeared step function, whose width δV_g should scale with temperature as \sqrt{T} , see Fig. 2.

V. LINEAR CONDUCTANCE AT A FINITE MAGNETIC FIELD

The magnetic field dependence of the linear conductance across the device also reveals the critical behavior. In this section we study the dependence $G(B)$ at $T=0$ in the vicinity of the quantum critical point $\Delta=0$. We consider only the Zeeman effect of the magnetic field, and dispense with its orbital effect (this is an adequate approximation for a field applied in the plane of a lateral quantum dot device).

Similar to the effect of a finite temperature, see Fig. 2, the application of a magnetic field at small Δ results in a crossover from the limiting FL behavior at $B \rightarrow 0$ to NFL intermediate regime at higher fields $B \gtrsim B_\Delta$. As before, the crossover scale B_Δ can be estimated¹⁸ from RG arguments. The scaling dimension²⁰ of the operator S^z in Eq. (10) at the 2CK fixed point is $1/2$. Accordingly, when the high energy cutoff D is lowered, the effective splitting of the impurity levels B^* evolves according to

$$\frac{B^*(D)/D}{B^*(T_K)/T_K} \propto \left(\frac{T_K}{D} \right)^{1/2} \quad (35)$$

with the initial condition $B^*(T_K) \sim B$. The RG flow Eq. (35) terminates once B^* has grown to become of the order of D , or when D reaches the value T_Δ , whichever occurs at a higher value of D . The first of the two conditions corresponds to the limitation on the NFL behavior set by the Zeeman splitting, while the second one is due to the channel anisotropy. Therefore, the crossover scale B_Δ can be estimated as that field $B \sim B^*(T_K)$ in Eq. (35), at which $B^*(D) \sim D$ and $D \sim T_\Delta$ simultaneously. Using Eqs. (35) and (31), we find the relation between the crossover field,⁶ the crossover temperature T_Δ , and the channel anisotropy parameter Δ

$$B_\Delta \sim \sqrt{T_\Delta T_K} \sim (|\Delta|/\mathcal{J}^2) T_K. \quad (36)$$

Note the difference between the Δ -dependence of the crossover temperature T_Δ [Eq. (31)] and the crossover field B_Δ .

Having found the crossover scale B_Δ , next we investigate the dependence of the conductance G on the field B . First of all, we note that at $\Delta \neq 0$ the low-energy properties of the Hamiltonian Eq. (10) are those of a Fermi liquid.⁴ The effect of any *local* perturbation, such as the exchange interaction with the spin of the dot 1 in Eq. (10), on the ground state of the Fermi liquid is completely characterized by the scattering phase shifts $\delta_{\gamma s}$ at the Fermi level. (Recall that $s = \pm 1$ for spin-up/down and $\gamma = 1, 2$ labels the two channels.) The t-matrix that enters Eq. (20) is then given by the standard scattering theory expression

$$-\pi\nu T_{\gamma s}(0) = \frac{1}{2i} (e^{2i\delta_{\gamma s}} - 1). \quad (37)$$

Obviously, the phase shifts are defined only mod π (that is, $\delta_{\gamma s}$ is equivalent to $\delta_{\gamma s} + \pi$). The ambiguity is removed by

setting the values of the phase shifts corresponding to $J_\gamma = 0$ in Eq. (10) to zero. With this convention, the invariance of the Hamiltonian (10) with respect to the particle-hole transformation $\psi_{\gamma ks} \rightarrow \psi_{\gamma, -k, -s}^\dagger$ translates into the relation

$$\delta_{\gamma s} + \delta_{\gamma, -s} = 0 \quad (38)$$

for the phase shifts, which suggests a representation

$$\delta_{\gamma s} = s \delta_\gamma. \quad (39)$$

Substitution of Eqs. (37) and (39) into Eq. (20) yields

$$G/G_0 = \frac{1}{2} \sum_s \sin^2 \delta_{1s} = \sin^2 \delta_1 \quad (40)$$

for the linear conductance at $T=0$. In the limit $B/T_K \rightarrow +0$ and at $\Delta \neq 0$, the ground state of the Hamiltonian (10) is a singlet. Therefore, the total spin in a very large but finite region of space surrounding the dot 1 is zero. By the Friedel sum rule, this implies relation $\sum_{\gamma s} s \delta_{\gamma s} = \pi$. Taking, in addition, Eq. (39) into account, one obtains relation

$$\delta_1 + \delta_2 = \pi/2, \quad (41)$$

valid at any value of B/B_Δ , as long as $B \ll T_K$.

Below the crossover, $B \ll B_\Delta$, the values of the phase shifts are determined by the vicinity of the stable Fermi-liquid fixed points,⁴ $\delta_1 = \pi/2$, $\delta_2 = 0$ at $\Delta > 0$ and $\delta_1 = 0$, $\delta_2 = \pi/2$ at $\Delta < 0$. Substitution of these values into Eq. (40) then yields Eq. (26) for the conductance. The corrections to the fixed point values of the phase shifts are linear in B/B_Δ ,

$$\delta_1 = \pi/2 - \delta_2 = (\pi/2) \theta(\Delta) - \text{sgn}(\Delta)(B/B_\Delta), \quad (42)$$

yielding

$$G/G_0 = \theta(\Delta) - \text{sgn}(\Delta)(B/B_\Delta)^2, \quad B \ll B_\Delta \quad (43)$$

[cf. Eq. (33)].

Above the crossover, i.e., for $B_\Delta \ll B \ll T_K$, the departure of the phase shifts from the 2CK fixed point values $\delta_{1,2} = \pi/4$ is controlled by the properties of the fixed point. To account for a finite value of B/T_K , we generalize Eq. (41):

$$\delta_1 + \delta_2 = \pi[1/2 + M(B)].$$

The zero-temperature magnetization $M(B)$ here is known exactly from the Bethe-ansatz solution.^{5,6,21} Using the asymptote²¹ $M(B) \propto (B/T_K) \ln(T_K/B)$, we find

$$\delta_1 = \frac{\pi}{4} + a \text{sgn}(\Delta) \frac{B_\Delta}{B} - b \frac{B}{T_K} \ln \frac{T_K}{B}. \quad (44)$$

Here a and b are positive numerical coefficients of the order of 1. The second term on the right-hand side of Eq. (42) is the first-order correction in the channel-symmetry-breaking perturbation. This correction is similar to Eq. (32) with temperature T replaced by the energy scale $D^*(B) \sim B^2/T_K$ at which the RG flow defined by Eq. (35) terminates. Equations (44) and (40) yield the asymptote of the conductance at $B_\Delta \ll B \ll T_K$,

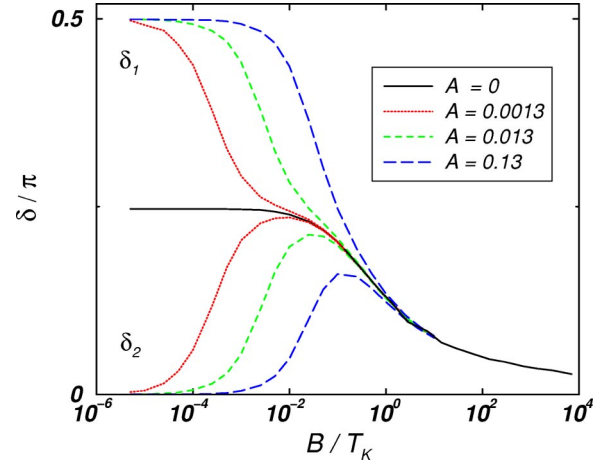


FIG. 4. The phase shifts for the 2CK model at different values of the channel asymmetry parameter $A = \Delta/\mathcal{J}^2$. The upper (lower) curves represent δ_1 (δ_2).

$$\frac{G}{G_0} = \frac{1}{2} + a \text{sgn}(\Delta) \frac{B_\Delta}{B} - b \frac{B}{T_K} \ln \frac{T_K}{B}. \quad (45)$$

The shape of $G(B)$ is qualitatively similar to that of $G(T)$, see Eqs. (23), (32), and (33), although the precise functional form is rather different.

Interestingly, in the case of small channel anisotropy, $T_\Delta \ll T_K$, there is an approximate symmetry with respect to the change of sign of Δ :

$$G(B, \Delta) + G(B, -\Delta) = 2G(B, \Delta \rightarrow 0). \quad (46)$$

Note that this relation is valid at any B/T_K , provided that $T_\Delta/T_K \ll 1$.

Strictly speaking, the consideration of this section is applicable only at zero temperature. However, the results Eqs. (43) and (45) remain valid⁹ as long as

$$T \ll B^2/T_K. \quad (47)$$

At higher temperatures the conductance is described by the corresponding expressions of Sec. IV. As follows from Eqs. (23) and (45), the limiting value of the linear conductance at the 2CK fixed point, $G = G_0/2$, is independent of the order in which the limits $B \rightarrow 0$, $T \rightarrow 0$ are taken.^{22,23} Hence, the crossover between the field-dominated regime, see Eqs. (43) and (45), and the temperature-dominated one, see Eqs. (23), (32), and (33), is expected to be smooth and featureless.

For arbitrary values of T_Δ/T_K , the detailed magnetic field dependence of the phase shifts at the Fermi level can be studied using the numerical renormalization group (NRG).²⁴ In this approach one defines a sequence of discretized Hamiltonians and diagonalizes them iteratively to obtain the finite-size spectrum of the model. In the Fermi liquid case ($\Delta \neq 0$) knowledge of the finite-size spectrum is sufficient to identify unambiguously the phase shifts.²⁰

In Fig. 4, we plotted the phase shifts $\delta_{1,2}$ as a function of B for different values of the parameter $A = \Delta/\mathcal{J}^2 > 0$ that characterizes the asymmetry between the channels. We estimate the crossover scales¹⁸ T_K and B_Δ as the two values of B in Fig. 4 at which the phase shift δ_2 equals $\pi/8$. In order to

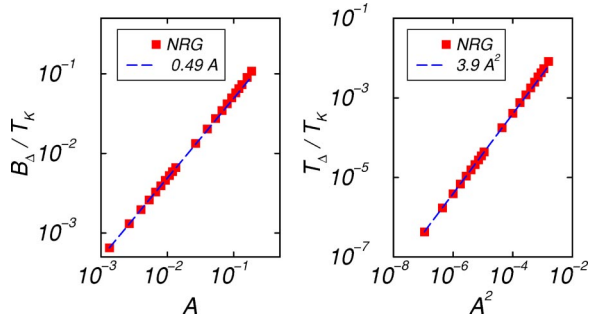


FIG. 5. Dependences of the crossover scales B_Δ and T_Δ on the asymmetry parameter $A = \Delta/\mathcal{J}^2$.

verify the relation $B_\Delta/T_K \sim A$, see Eq. (36), we plotted B_Δ vs A on the left panel in Fig. 5. The NRG data also allow us to estimate the scale T_Δ , see Eq. (31), as the energy scale at which the first excited state of the NRG spectrum has reached the halfway mark of its crossover evolution between the corresponding two fixed point values, see Fig. 5, right panel. The NRG data are very well described by $B_\Delta/T_K \approx 0.5A$, $T_\Delta/T_K \approx 4A^2$, in agreement with Eqs. (36) and (31) above.

Having extracted the phase shifts, we are able to calculate the linear conductance from Eqs. (40) and (46), see Fig. 6. As expected, the conductance develops a signature of a plateau at intermediate values of the field $B_\Delta < B < T_K$. At very high fields, $B \gg T_K$, the conductance scales with B as $1/\ln^2(B/T_K)$.

As usual in NRG calculations, we measured all energies in units of the bandwidth D . In order to avoid the disturbing finite bandwidth effects, we used two different coupling constants for the high- and low-field regimes: one set of data, that includes the $B \gg B_\Delta$ regime, was obtained using $\mathcal{J} = 0.075$, while another set of data, which includes the $B \ll T_K$ regime, was obtained using $\mathcal{J} = 0.15$. The two sets were combined by rescaling the magnetic field in units of the Kondo temperature, resulting in a set of continuous curves, as shown in the figures. The overlap of the two sets of data at

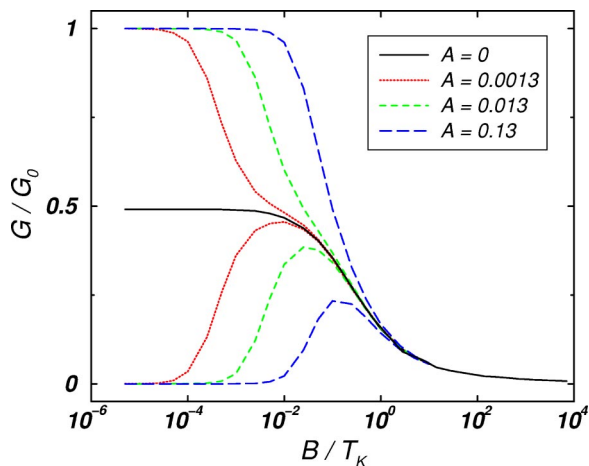


FIG. 6. Field dependence of the conductance at different values of the asymmetry parameter $A = \Delta/\mathcal{J}^2$. The upper (lower) curves correspond to $A > 0$ ($A < 0$).

intermediate fields confirms that in this regime the accuracy of our numerics is remarkably good. Based on the dependence on the finite system size, we estimate the relative error of the calculated phase shifts to be of the order of 2%. (The worst case is the low field part of the $A = 0$ curve, because of the extremely fragile nature of the intermediate NFL fixed point.)

VI. EFFECT OF POTENTIAL SCATTERING

So far we concentrated on the particle-hole symmetric model. In general, however, such symmetry is absent. It is violated by the presence of higher energy levels in dot 1, and also by deviations of the dimensionless gate voltage N from an integer value. In the absence of particle-hole symmetry, the effective Hamiltonian (10) acquires additional terms leading to potential scattering. Taking into account that the interchannel scattering is blocked at energies well below $E_{1,2}$, we can write this additional perturbation as

$$H_p = \sum_{\gamma=1,2} V_\gamma \sum_{kk's} \psi_{\gamma ks}^\dagger \psi_{\gamma k' s}. \quad (48)$$

Including H_p into our considerations leads to a modification of the limiting values of the conductance in the Fermi-liquid and 2CK fixed points. The dependences of dI/dV on Δ , V , T and B , however, remain the same apart from acquiring a constant background contribution G_{el} due to elastic cotunneling. Here we illustrate this for a specific example of the zero-temperature magnetoconductance.

The potential scattering yields finite spin-independent phase shifts $\delta_\gamma^0 = -\arctan(\pi\nu V_\gamma)$ even if J_γ in Eq. (10) are set to 0. This can be accounted for by a proper modification²⁵ of Eq. (39),

$$\delta_{\gamma s} = \delta_\gamma^0 + s \delta_\gamma, \quad (49)$$

where the dependence of δ_γ on B and Δ is described by the ‘‘particle-hole symmetric’’ expressions (42) and (44). Substitution of the phase shifts in the form of Eq. (49) into Eq. (40) results in¹⁵

$$G(B, \Delta) = G_{el} + \tilde{G}_0 F[B/B_\Delta, B/T_K, \text{sgn}(\Delta)], \quad (50)$$

where $G_{el} = G_0 \sin^2 \delta_1^0$, the function F is a universal function with asymptotes given in Eqs. (43) and (45), and $\tilde{G}_0 = G_0 - 2G_{el}$. Note that the limiting value of the conductance at the 2CK fixed point, $G_{el} + \tilde{G}_0/2$, lies precisely *halfway* between the two Fermi-liquid limits, G_{el} and $G_{el} + \tilde{G}_0$, and that Eq. (46) remains valid even in the presence of the potential scattering Eq. (48).

VII. DISCUSSION

The low-temperature properties of a quantum dot device normally are well described by Fermi liquid theory. The special two-dot structure proposed in Ref. 17 allows, however, for NFL behavior at a special point in the space of parameters of the device. In the context of the physics of quantum phase transitions, this point can be viewed as a critical point

separating two Fermi liquid states. In this paper, we developed a detailed theory of the transport properties near such a quantum critical point. Our theory offers a strategy for tuning the device parameters to the critical point characterized by the two-channel Kondo effect physics, by monitoring the temperature dependence of the linear conductance, see Sec. IV. Further confirmation of the 2CK behavior may come from the measurements of the differential conductance, which must display universal behavior, see Sec. IV. We also investigated the effect of magnetic field and of potential scattering on the conductance in the vicinity of the quantum critical point, see Secs. V and VI. The Zeeman splitting allows one to investigate the finite-field crossover between the Fermi liquid and NFL behavior of the conductance. In the vicinity of the NFL point, the linear conductance of the device depends on the magnetic field and temperature only via two dimensionless parameters T/T_Δ and B/B_Δ ; the dependence of T_Δ and B_Δ on the channel asymmetry Δ is given in Eqs. (31) and (36). Note also that potential scattering does

not destroy the 2CK behavior, but merely renormalizes the magnitude of the Kondo contribution to the conductance. A finite level spacing in the larger dot δE_2 , however, is a hazard. At temperatures below δE_2 the two-dot device inevitably enters into the conventional Fermi-liquid regime.

ACKNOWLEDGMENTS

We are grateful to the Aspen Center for Physics, Max Planck Institute for the Physics of Complex Systems (Dresden), and LMU München for hospitality and thank N. Andrei, A. Ludwig, Y. Oreg, A. Rosch, A. Tsvetlik, and G. Zaránd for discussions. The research at the University of Minnesota was supported by NSF Grants Nos. DMR02-37296 and EIA02-10736. L.B. acknowledges the financial support provided through the European Community's Research Training Networks Program under Contract No. HPRN-CT-2002-00302, Spintronics.

¹P.W. Anderson, *Basic Notions of Condensed Matter Physics* (Addison-Wesley, Reading, 1997).

²P. Nozières, *J. Low Temp. Phys.* **17**, 31 (1974).

³A.I. Larkin and V.I. Melnikov, *Zh. Éksp. Teor. Fiz.* **61**, 1231 (1971) [*Sov. Phys. JETP* **34**, 656 (1972)].

⁴P. Nozières and A. Blandin, *J. Phys. (France)* **41**, 193 (1980).

⁵P.B. Wiegmann and A.M. Tsvetlik, *Pis'ma Zh. Éksp. Teor. Fiz.* **38**, 489 (1983) [*JETP Lett.* **38**, 591 (1983)]; A.M. Tsvetlik and P.B. Wiegmann, *J. Phys. C* **17**, 2321 (1983); A.M. Tsvetlik, *ibid.* **18**, 159 (1985); N. Andrei and C. Destri, *Phys. Rev. Lett.* **52**, 364 (1984).

⁶N. Andrei and A. Jerez, *Phys. Rev. Lett.* **74**, 4507 (1995).

⁷A.M. Tsvetlik, *J. Phys.: Condens. Matter* **2**, 2833 (1990).

⁸I. Affleck and A.W.W. Ludwig, *Phys. Rev. B* **48**, 7297 (1993).

⁹D.L. Cox and A. Zawadowski, *Adv. Phys.* **47**, 599 (1998).

¹⁰I.L. Aleiner, B.L. Altshuler, Y.M. Galperin, and T.A. Shutenko, *Phys. Rev. Lett.* **86**, 2629 (2001).

¹¹K.A. Matveev, *Phys. Rev. B* **51**, 1743 (1995); K.A. Matveev, *Zh. Éksp. Teor. Fiz.* **99**, 1598 (1991) [*Sov. Phys. JETP* **72**, 892 (1991)].

¹²L.I. Glazman, F.W.J. Hekking, and A.I. Larkin, *Phys. Rev. Lett.* **83**, 1830 (1999).

¹³A. Furusaki and K.A. Matveev, *Phys. Rev. B* **52**, 16 676 (1995).

¹⁴D. Goldhaber-Gordon, H. Shtrikman, D. Mahalu, D. Abusch-Magder, U. Meirav, and M.A. Kastner, *Nature (London)* **391**, 156 (1998); S.M. Cronenwett, T.H. Oosterkamp, and L.P. Kouwenhoven, *Science* **281**, 540 (1998); J. Schmid, J. Weis, K. Eberl, and K. von Klitzing, *Physica (Amsterdam)* **256B-258B**,

182 (1998); W.G. van der Wiel, S. De Franceschi, T. Fujisawa, J.M. Elzerman, S. Tarucha, and L.P. Kouwenhoven, *Science* **289**, 2105 (2000).

¹⁵M. Pustilnik and L.I. Glazman, *Phys. Rev. Lett.* **87**, 216601 (2001).

¹⁶L.I. Glazman and M. Pustilnik, in *New Directions in Mesoscopic Physics (Towards Nanoscience)*, edited by R. Fazio, V.F. Gantmakher, and Y. Imry (Kluwer, Dordrecht, 2003), pp. 93–115.

¹⁷Y. Oreg and D. Goldhaber-Gordon, *Phys. Rev. Lett.* **90**, 136602 (2003).

¹⁸The definitions of the crossover scales T_K , T_Δ , and B_Δ adopted in this paper are based on the asymptotic behavior of the linear conductance at low T and B , see Eqs. (23), (33), and (43), correspondingly.

¹⁹S. Sachdev, *Quantum Phase Transitions* (Cambridge University Press, Cambridge, 1999).

²⁰I. Affleck, A.W.W. Ludwig, H.-B. Pang, and D.L. Cox, *Phys. Rev. B* **45**, 7918 (1992).

²¹P.D. Sacramento and P. Schlottmann, *Phys. Rev. B* **43**, 13 294 (1991).

²²Note that if the number of channels is larger than 2, the value of the conductance at $T \rightarrow 0$ and $B \rightarrow 0$ depends on the order in which the limits are taken. This property is easy to understand in the limit of very large number of channels when the NFL fixed point lies within the reach of perturbation theory (Refs. 4,8,23).

²³S. Florens and A. Rosch, cond-mat/0311219 (unpublished).

²⁴K.G. Wilson, *Rev. Mod. Phys.* **47**, 773 (1975).

²⁵P. Nozières, *J. Phys. (France)* **39**, 1117 (1978).